Effect of Various Sizes of Calcined Marsh Clam Shell on Phosphate Removal from Aqueous Solution

Noorul Hudai Abdullah[1,*], Muhammad Azreen Mohd Azmi[2], Muhammad Afham Mohd Zaidi[2], Nur Balqis Nasaruddin[2], Nur Atikah Abdul Salim[3], Nur Hanis Hayati Hairom[4,5], Muhammad Faris Abdul Hadi[4,5], Mohamad Ali Fulazzaky[6]

[1] Neo Environmental Technology, Centre for Diploma Studies, Universiti Tun Hussein Onn Malaysia, Pagoh Education Hub, 84600 Pagoh, Johor, Malaysia
[2] Centre for Diploma Studies, Universiti Tun Hussein Onn Malaysia, Pagoh Education Hub, 84600 Pagoh, Johor, Malaysia
[3] School of Civil Engineering, Faculty of Engineering, Universiti Teknologi Malaysia, 81310 UTM Johor, Malaysia
[4] Microelectronics and Nanotechnology-Shamsuddin Research Center, Institute for Integrated Engineering, Universiti Tun Hussein Onn Malaysia, Parit Raja, 86400 Batu Pahat, Johor, Malaysia
[5] Faculty of Engineering Technology, Universiti Tun Hussein Onn Malaysia, Hab Pendidikan Tinggi Pagoh, Km 1, Jalan Panchor, 84600 Muar, Johor, Malaysia
[6] School of Postgraduate Studies, Universitas Djuanda, Jalan Tol Ciawi No. 1, Ciawi, Bogor 16720, Indonesia

ARTICLE INFO

ABSTRACT

Phosphorus is one of essential elements for sustaining life largely through phosphate, a compound containing the phosphate ion, PO_4^{3-}. However, excessive phosphorus concentrations will cause eutrophication and this condition is considered as an environmental issue. The phosphorus sources are commonly from human activities; for instance, detergents, fertilisers, and industries. Although various adsorption techniques have been applied to remove phosphorus in water, the effect of different particle sizes of calcined marsh clam shells on phosphate removal has not been fully investigated, along with its adsorption kinetics and isotherms. This study investigates phosphate removal from synthetic solution onto calcined marsh clam shells (CMCs) with 5 different particle sizes: 0.075–0.15, 0.15–0.30, 0.30–0.60, 0.60–1.18, and 1.18–2.36 mm. The batch experiment used 2 g of adsorbent and synthetic potassium dihydrogen phosphate (KH_2PO_4) solution. The adsorbent size of 0.075 to 0.15 mm showed the highest removal (100%) efficiency due to high adsorption rate. The experimental data were further analysed using kinetics and isotherm models; the data fitted well with pseudo-second-order kinetic model (R^2 = 0.9986) and Freundlich isotherm model (R^2 = 0.8404). The potential of marsh clam shells as an adsorbent for phosphate removal in water is significant for future applications in wastewater treatment technology.

1. Introduction

The abundance of nutrient pollutants is becoming a serious environmental issue worldwide due to the rapid increase of industries, metropolitan areas, and contemporary agricultural activities. The

---

* Corresponding author.
E-mail address: noorul@uthm.edu.my

most prevalent anions, such as phosphate and nitrate, are essential elements found in insecticides, fungicides, fertilizers, and agricultural products. Excess phosphorus in water bodies encourages plant growth, lowers water quality, generates algal blooms, kills aquatic life, and results in eutrophication [1]. Eutrophication is a term used to describe an increase in phosphorus levels as a result of human activities, which will have an impact on ecosystems around the world in the next decades [2]. Water bodies may also lose important functions, leading in significant environmental and human health repercussions. Phosphate ions have been found in a variety of primary and secondary sources, including industrial waste, sewage sludge, household trash, and surface waterways. Phosphorus is not completely removed from wastewater using standard procedures. According to the European Union (EU) and the United States Environmental Protection Agency (USEPA), uncontrolled phosphorus discharge into surface waters could lead to legal concerns. The EU authorizes a discharge limit of 2 mg/L per 100,000 population equivalents, while the USEPA allows a total phosphorus effluent limit of less than 0.8 mg/L [3].

Chemical precipitation, biological treatment, membrane separation, and adsorption are some of the phosphorus removal approaches developed in recent years to remove excess phosphorus. Because of its high effectiveness, ease of operation, and economic value, adsorption is usually recognized as a great and promising solution for removing phosphorus from polluted water. Some adsorbents are made from discarded shells and have the ability to extract phosphorus from water due to the calcium carbonate content [4]. The large amount of waste shell like marsh clam shell from domestic waste can pose environmental issues. To help minimize or avoid eutrophication, calcined marsh clam shells (CMCs) have the potential to remove phosphorus from solutions. This study focuses on CMC particle sizes in the range of 0.075–0.15, 0.15–0.30, 0.30–0.60, 0.60–1.18, and 1.18–2.36 mm. The adsorbent was calcined at 800°C to increase the pore size of the surface material. Kinetics and isotherm models were applied to verify the data fit with the experiment. This study's contribution is to improve alternative wastewater treatment technology by utilizing environmentally friendly materials. The goal of this study is to investigate the removal of phosphorus from synthetic solutions through CMCs with various particle sizes. Evaluate and compare the removal efficiency of five different adsorbent sizes was evaluated and compared based on batch experiment data and the data was verified with kinetics and isotherm adsorption models.

2. Material and Methods
2.1 Preparation of Adsorbent

The marsh clam shells were collected from Kelantan, Malaysia. The shells were cleaned and dried for 2 days at 30 °C. The shells were then crushed and sieved for 5 different ranges of particle sizes which were 0.075–0.15, 0.15–0.30, 0.30–0.60, 0.60–1.18, and 1.18–2.36 mm. The adsorbents were calcined for 2 h in an 800°C furnace.

2.2 Preparation of Aqueous Solution

In this batch study, potassium dihydrogen phosphate (KH_2PO_4) was used as the chemical component to represent phosphorus in wastewater. The solution concentration was kept constant at 10 mg/L and it was prepared by dissolving 0.1433 g of KH_2PO_4 in 1.0 L of deionized water.

2.3 Batch Experiment

In the batch experiment, 2 g absorbent was added to a 100 mL (KH_2PO_4) solution in a conical flask for 10 flasks and shaken using an orbital shaker at 170 rpm for interval time 5, 10, 15, 20, 25, 30, 40, 50, 65, and 95 minutes. The samples were filtered to remove the suspended matters and analyzed using UV–vis spectrophotometer (HACH DR6000) to measure the final phosphate content with wavelength is 530 nm for spectrophotometers [5].

2.4 Analytical Method

A scanning electron microscope (SEM; COXEM EM-30AX PLUS SEM) was used to assess the porosity and surface morphology of the CMCs, while the chemical and percentage contents were measured using energy dispersive X-ray fluorescence (EDXRF). A Fourier transform infrared spectrometer (FTIR; Perkin Elmer Spectrum Two FTIR) was used to investigate phosphate adsorption functional group before and after CMCs treatment. The crystal phase composition of the adsorbent was determined using X-ray diffraction (XRD; Second Generation BRUKER D2 Phaser).

3. Results
3.1 Characterization of Physical and Chemical Properties

Changes in the surface and porosity of the materials after adsorption process were assessed using SEM with EDXRF. The functional groups present and any changes in peak location and intensity were assessed using FTIR before and after adsorption. The structural alterations and formation of new crystallographic structures after phosphate adsorption were determined using XRD analyses.

3.1.1 SEM and EDXRF analysis

Due to calcite and lime particles, the calcite and lime particles formed various grooves and ridges on the surface, which are useful for adsorption. A distinct crystal-like architecture is seen in the twisted particle accumulations of CMCs particles. Thermal activation revealed surface fissures. The SEM images of the shells at are shown in Figure 1, where the calcined marsh clam shells show a crystal-like texture and high porosity.
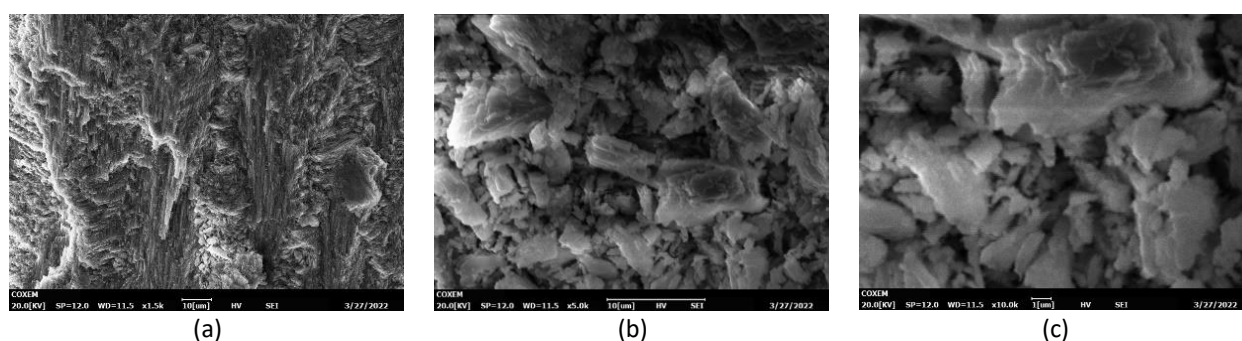

(a)   (b)   (c)
Fig. 1. SEM photomicrograph of CMCs at (a) 1500×, (b) 5000×, and (c) 10000× magnification

EDXRF was used to evaluate the elemental compositions of CMCs. The elemental makeup of CMCs is shown in Table 1. Ca and O were the most abundant components in the CMCs, with 29.83% Ca and 51.10% O detected. Materials containing Ca have the ability to remove phosphate from an

aqueous solution in most cases [6]. As a result, CMCs may be able to adsorb phosphate from aqueous solutions.

Table 1
Elemental composition of calcined marsh clam shells

Element	Weight (%)
Ca	29.83
O	51.10
C	15.54
Au	3.13
Na	0.40

3.1.2 FTIR analysis

The functional groups present on the surface of the adsorbent were investigated using FTIR. The bands at roughly 3700–800 cm^{-1} confirm the presence of the common inorganic ions in CMCs as shown in Figure 2 [6]. The position and shape of the phosphate stretching band in the FTIR spectra of the marsh clam shell are influenced by the nature and position of the surface functional groups. Before phosphate adsorption, the two bands at 1407.11 and 869.32 cm^{-1} confirm the presence of carbonate ion [7]. Two bands have a significant change from 3640.85 and 1407.11 cm^{-1} before adsorption to 3640.49 and 1412.48 cm^{-1}, respectively, after adsorption of phosphate from aqueous solution onto the CMCs. The difference in the frequency spectrum of 0.36 cm^{-1} (3640.85 − 3640.49 cm^{-1}) is because the O–H stretching bands at the CMC surface are affected by asymmetric stretching mode of vibration from the phosphate group [8]. The phosphate molecules adsorbed onto the surface of CMCs may have caused the increase by 5.37 cm^{-1} (1407.11 − 141248 cm^{-1}) due to inorganic carbonate ion [9].
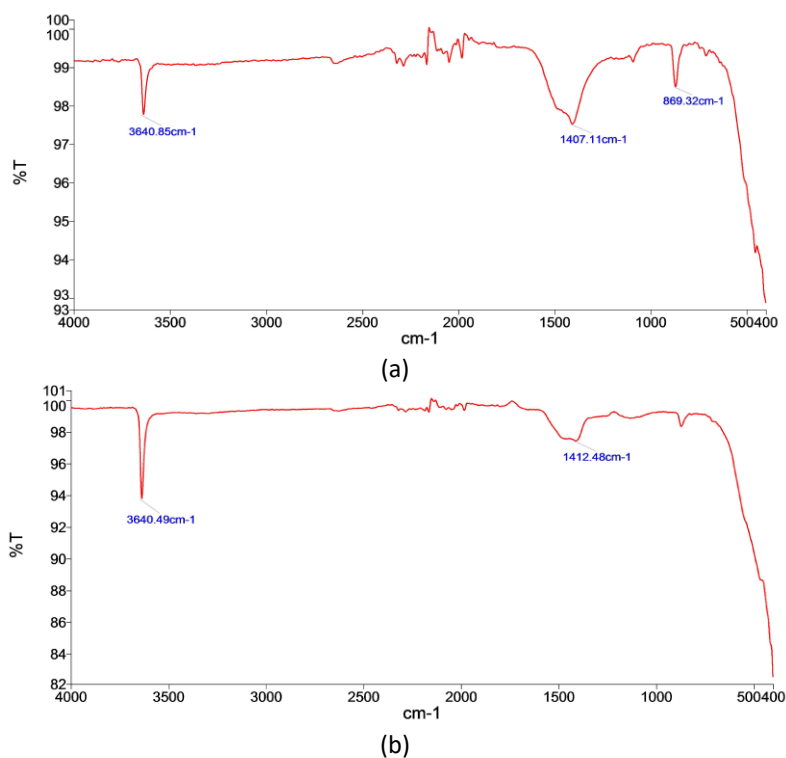

Fig. 2. FTIR spectra of (a) before and (b) after adsorption

3.1.3 XRD analysis

Structural changes caused by unique crystallographic structures induced by phosphate adsorption were detected using XRD as shown in Figure 3 [10]. Calcination of crushed marsh clam shells resulted in considerable changes in the chemical and crystal characteristics of the raw material, yielding CMCs that were largely constituted of Lime 48% and Portlandite 62% [11].
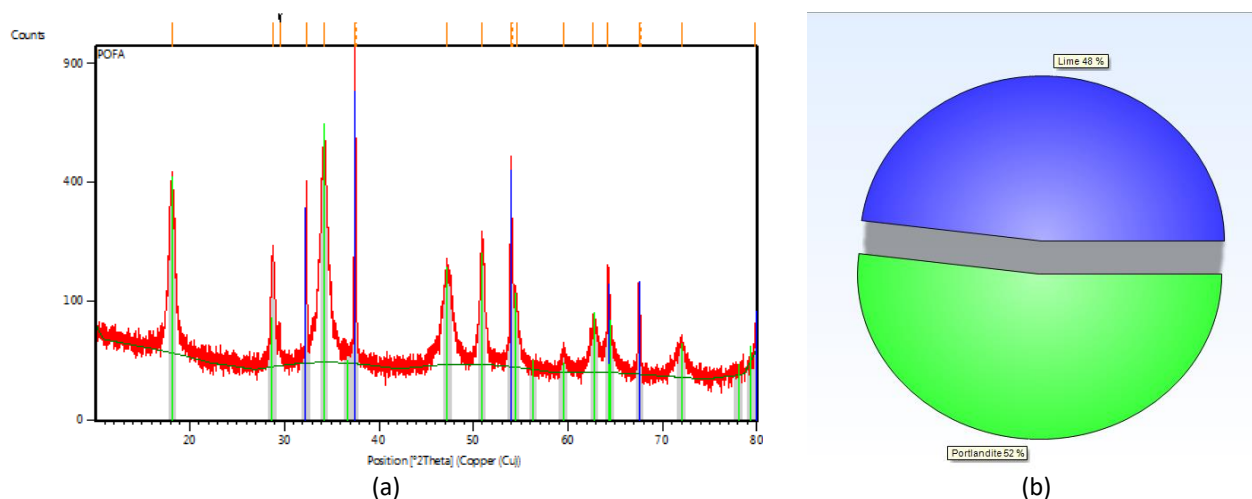

| (a) | (b) |

Fig. 3. XRD diffraction patterns of (a) pattern of graphic and (b) distribution of component in CMCs

3.2 Removal Efficiency, E (%) for Various Particle Sizes

The effect of various particle sizes of CMCs in the range of 0.075–0.15, 0.15–0.30, 0.30–0.60, 0.60–1.18, and 1.18–2.36mm on phosphate removal efficiency was investigated, and the results are shown in Figure 4. The phosphate removal efficiency by CMCs with particle size 0.075–0.150 mm was the highest (100%). The phosphate removal efficiency increased as the time was increased. The particle size of 0.075–0.015 mm recorded the highest removal efficiency because a smaller adsorbent size results in a higher surface area, providing more sites for phosphate adsorption from the aqueous solution [12].

The CMCs with particle size 0.15–0.30 mm had the second-highest absorption efficiency at 96.96%. CMCs with particle size ranging from 1.18 to 2.36 mm had the lowest phosphate removal efficiency, which was 92.27%. This is because a bigger particle size gives a smaller contact surface area per volume [13]. This suggests that phosphate was incorporated into the material after adsorption. According to the XRD data, calcite and lime crystals can micro precipitate $P–PO_4^{3-}$ [14,15]. The intensity of the first XRD peaks of pure CMCs decreased after phosphate adsorption.
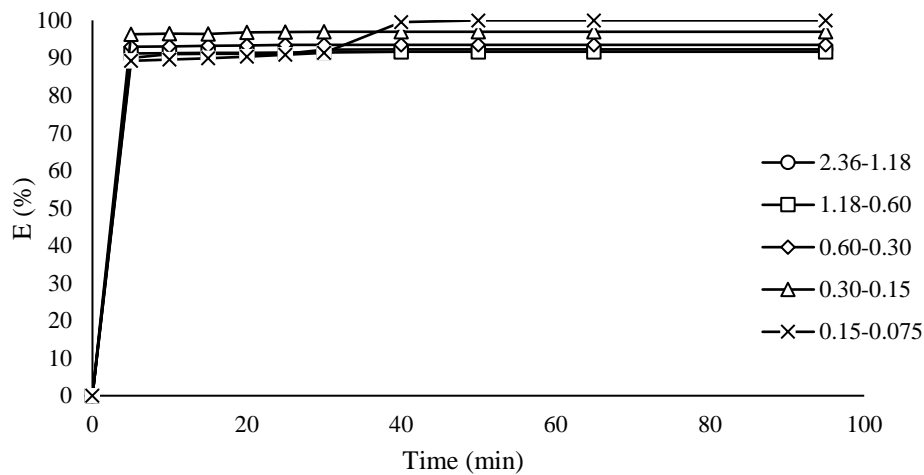
Fig. 4. Removal efficiency, E (%) for various particle size

3.3 Adsorption Capacity, q (mg/g) for Various Particle Sizes

The contact time for the different sizes of CMCs is the primary effect of the adsorption capacity in the CMCs. The capacity for accommodation increased in direct proportion to the length of time required for the process of adsorption. As shown in Figure 5, initially the capacity to adsorb phosphate was relatively low; however, as the reaction time was increased, the adsorption capacity also increased. The most important factor in determining the adsorption capacity of CMCs is the adsorbent's particle size [16]. According to the various particle sizes of calcined CMCs, which range from 0.075–0.15, 0.15–0.30, 0.30–0.60, 0.60–1.18, and 1.18–2.36mm. The batch experiment was carried out to measure the adsorption capacity (Figure 5) of each sample and determine which adsorbent size resulted in the highest phosphate removal.

The adsorption capacity of CMCs with particle size of 0.075–0.15 mm was the highest when compared to other particle sizes. Figure 5(e) displays the adsorption capacity of CMCs with a particle size of 0.075–0.15 mm, which attained the maximum q value of 0.534 mg/g. The EDX analysis showed a rise in calcium concentration. The FTIR spectra of the adsorbents display significant variations before and after the adsorption process. After the phosphate adsorption process, the strength of the carbonate peaks was altered, indicating the loss of carbonate and the formation of new phosphate minerals [17,18]. This suggests that phosphate was incorporated into the material after adsorption. Based on the results of our XRD investigation (Figure 3), both lime and portlandite are capable of micro precipitating $P–PO_4^{3-}$ [19]. After phosphate adsorption, the strength of the initial XRD peaks detected in pure CMCs was diminished. It is feasible to calculate the adsorption capacity using the formula in Eq. (1).

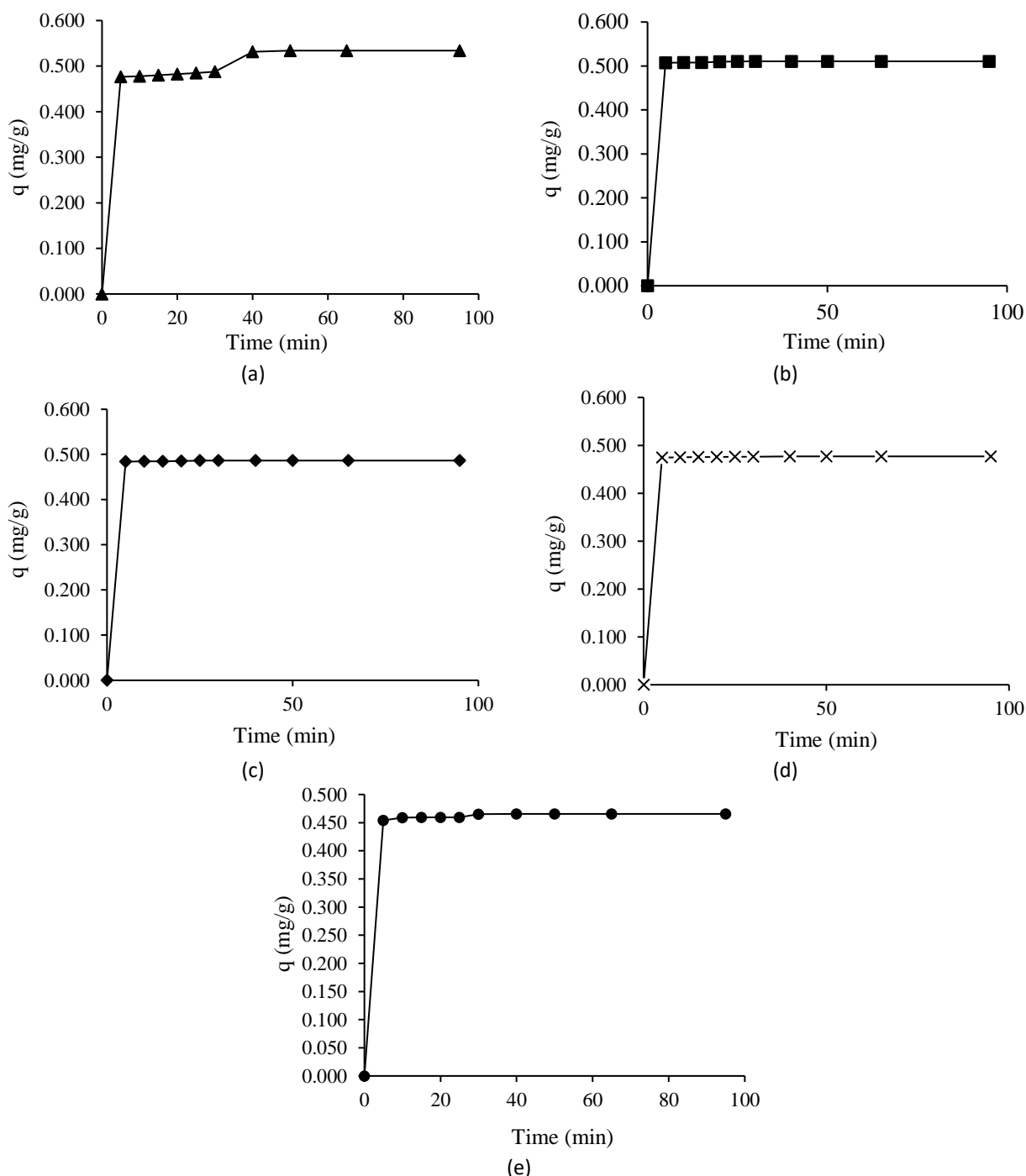$$q = \frac{(c_i - c_f) \times V}{m} \qquad (1)$$

Fig. 5. Adsorption capacity, q (mg/g) for (a) 0.075–0.15, (b) 0.15–0.30, (c) 0.30–0.60, (d)0.60–1.18, and (e) 1.18–2.36mm

3.4 Adsorption Kinetics for CMCs with Various Particle Sizes

Models of adsorption kinetics indicate the pace and mechanism of response in the adsorption mechanism and the change from a liquid to a solid state [20]. Previous research developed pseudo-first-order (PFO) and pseudo-second-order (PSO) kinetic models for ion adsorption from solution [21]. The amount of time necessary to achieve adsorption equilibrium is one of the most important design requirements for an expense wastewater treatment system [22]. Thus, Eq. (2) and Eq. (3) were used as the linear equation of the graph to display the PFO and PSO kinetic model.

$$\ln[q_e - q_t] = \ln q_e - k_1 t \tag{2}$$

$$\frac{t}{q_t} = \frac{t}{q_e} + \frac{1}{k_2 q_e^2} \tag{3}$$

where q_e is the quantity of phosphate that has been adsorbed at equilibrium (mg/g), q_t is the quantity of phosphate that has been adsorbed at a specific time (mg/g), k_1 (min^{-1}), and k_2 (g.mg^{-1}.min^{-1}), are constants that represent the rate of the PFO and PSO equation and t is the amount of time that has passed since the beginning of the adsorption process (min) [23]. After that, in relation to the value of the parameter error function, F_e as shown in Eq. (4).

$$F_e = \sqrt{\left(\frac{1}{n-p}\right) \sum_i^n (q_{t\ (exp)} - q_{t\ (theo)})^2} \tag{4}$$

where n refers to the total number of measurements, p stands for the number of kinetic parameters, $q_{t(exp)}$ stands for the value of q obtained via experimentation, and $q_{t(theo)}$ stands for the value of q obtained through theory (mg/g). The model with the lowest Fe value and the greatest R^2 value should be considered the most suitable option [24].

The PFO and PSO models were used to derive conclusions from the experimental data [25]. The values of the kinetic parameters for both models, which are adsorption capacity (q), rate constant (k), correlation coefficient (R^2), and error function (F_e), are shown in Table 2. The q_e value that was generated from the PFO model was considerably different from the q_e value that was determined from the experimental data, but the q_e value that was produced from the PSO model was consistent with that from the experimental data [26]. The R^2 values varied from 0.9974 to 0.9986, and the PSO plot is made up entirely of straight lines (t/q_t versus t) [27]. The R^2 values obtained from the PFO model varied from 0.4802 to 0.6913 and were lower than those obtained from the PSO. Table 2 and Figure 6 show the values of q_e and R^2. The fitting curves in Figure 6 and the kinetic parameters in Table 2 reveal that the PSO kinetic model is better suited for predicting the kinetics of phosphate adsorption onto CMCs. This demonstrates that the chemisorption mechanism regulates the overall rate of the phosphate adsorption process, which includes the exchange of electrons, covalent bonds, and ions [28,29].

In addition, the phosphate ions that were investigated for this research were shown to be in close proximity to the active sites during the first stages of the kinetics process. After this amount of time, equilibrium is achieved as a result of electro repulsion between the ions that are adsorbed onto the adsorbent surface and the ions that are in the solution [30].

Table 2
Kinetic parameters of pseudo-first-order model and pseudo-second-order models

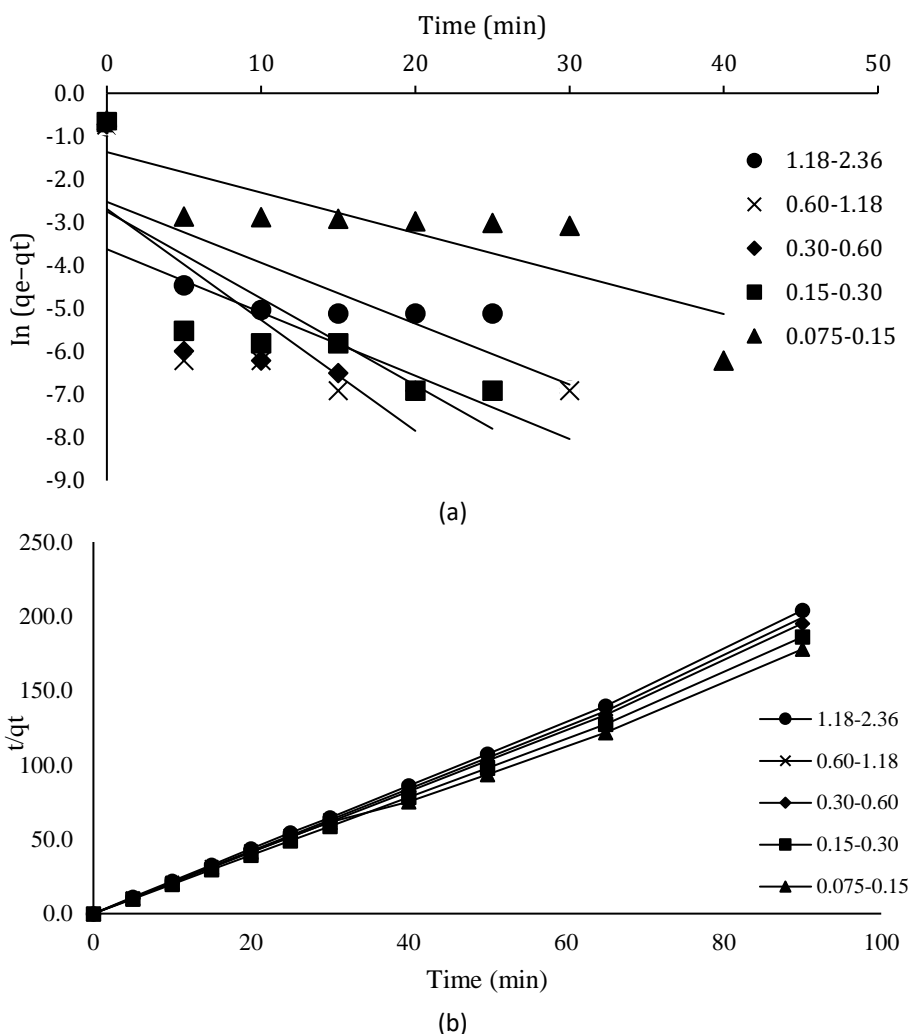| Particle Size	Pseudo-First-Order Model					Pseudo-Second-Order Model				
	$q_{e(theo)}$	k_1	R^2	F_e	$q_{e(exp)}$	$q_{e(theo)}$	k_2	R^2	F_e	$q_{e(exp)}$
1.18–2.36	0.0802	0.1415	0.6666	4.7688	0.466	0.4491	−3.8019	0.9985	17.7075	0.466
0.60–1.18	0.0267	0.1470	0.4904	5.3456	0.477	0.4595	−3.1064	0.9986	12.8629	0.477
0.30–0.60	0.0679	0.2577	0.6310	5.9465	0.487	0.4686	−2.9808	0.9986	15.5367	0.487
0.15–0.30	0.0641	0.2019	0.6571	5.7968	0.511	0.4919	−2.8889	0.9986	18.8008	0.511
0.075–0.15	0.2548	0.0941	0.6913	3.4115	0.534	0.5219	−2.6774	0.9974	0.0000	0.534

Fig. 6. (a) Pseudo-first-order and (b) Pseudo-second-order graphs (Linear regression study for the adsorption of PO_4^{3-} onto an adsorbent from a synthetic solution)

3.5 Adsorption Isotherms for CMCs with Various Particle Sizes

For the investigation of the adsorption isotherms of phosphate onto CMCs for every particle size, the batch experiment data were fitted to the Langmuir and Freundlich models. Table 3 lists all the parameter values calculated using these two isotherm models. The Freundlich isotherm model has a larger R^2 value (0.8404) and thus fits the experimental data better than the Langmuir isotherm model ($R^2 = 0.8236$). This is because, at the smallest particle size of adsorbent 0.075–0.15 mm, the Freundlich isotherm model represented the adsorption process with a higher coefficient of determination R^2 than the Langmuir isotherm model. The Freundlich isotherm model best suits the batch experiment data analysis when the values of amount of phosphorus removal from solution are predicted [31]. As illustrated in Figure 7, the correlation is fitted accordingly.

Table 3
Parameter of isotherm model for the adsorption of PO_4^{3-}

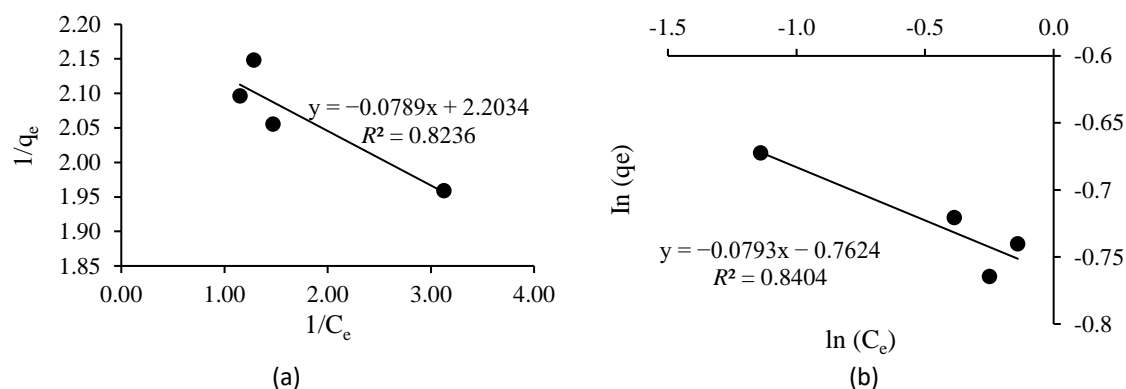| Freundlich Model			Langmuir Model		
n	K_F	R^2	q_{max}	K_L	R^2
−12.6103	0.4665	0.8404	0.4538	−27.9292	0.8236

Fig. 7. (a) Langmuir and (b) Freundlich adsorption isotherms for CMCs

Based on the results of a batch experiment that was conducted and computed using kinetic and isotherm models, the results of this study reveal that CMC is capable of adsorbing phosphate from the synthetic solution. The adsorbent with 0.075–0.15 mm particle size recorded the best adsorption capacity, q_e (0.534 mg/g), and removal efficiency, E (100%). This is due to the significant affinity between calcium oxide on the surfaces of CMCs and phosphate ions, which is because both molecules have different charges, making them attract one another [32]. Furthermore, the phosphate adsorption efficiency rates onto CMCs (0.075–0.15 mm) was the highest and required only 50 min to achieve equilibrium compared to the other CMCs with bigger particle sizes, which took a shorter time to reach equilibrium but had lower adsorption efficiency [33]. This is because the calcination process alters the physical and chemical properties of the adsorbent by changing the calcium carbonate. At 600–800 °C, calcium carbonate transforms into calcium oxide [34]. This is corroborated by the Figure 1 in the section on characterization of physical and chemical properties of the adsorbent, which illustrates the porosity of the adsorbent and the crystal-like texture and small pores in the CMC structure.

4. Conclusions

In conclusion, calcined marsh clam shells could be utilized as an adsorbent to extract phosphate from an aqueous solution. The highest removal efficiency was reached at an adsorbent particle size of 0.075–0.15 mm with a 100% removal efficiency. The lowest removal efficiency was 92.27% with the adsorbent particle size 1.18–2.36 mm. This is consistent with the hypothesis that a smaller adsorbent size results in higher surface area for phosphate adsorption in the aqueous solution, thus increasing the removal efficiency of phosphate by CMCs. The adsorption kinetic data best fitted the PSO model due to highest correlation coefficient (R^2 = 0.9974), demonstrating that chemisorption regulates the overall rate of the phosphate adsorption process, which includes the exchange of electrons, covalent bonds, and ions. The isotherm model data were well fitted with Freundlich isotherm model (R^2 = 0.8404), demonstrating that phosphate adsorption onto CMCs occur on a heterogeneous surface with multilayer sorption. The potential of CMCs as an alternative adsorbent for phosphate removal in water is significant for future applications in wastewater treatment technology.

References

[1] Abdullah, Noorul Hudai, Nur Amirah Adnan, Nur Fatin Nadiah Mohd Rashidi, Mohamad Syahrul Syazwan Yaacob, and Nur Atikah Abdul Salim. "Comparing the adsorption isotherms and kinetics of phosphate adsorption on various waste shells as adsorbent." *Water Practice & Technology* 17, no. 5 (2022): 974-985. https://doi.org/10.2166/wpt.2022.051

[2] Karthikeyan, Perumal, P. Sirajudheen, Manuvel Raja Nikitha, and Sankaran Meenakshi. "Removal of phosphate and nitrate via a zinc ferrite@ activated carbon hybrid composite under batch experiments: study of isotherm and kinetic equilibriums." *Environmental Nanotechnology, Monitoring & Management* 14 (2020): 100378. https://doi.org/10.1016/j.enmm.2020.100378

[3] Salim, Nur Atikah Abdul, Mohamad Ali Fulazzaky, Mohd Hafiz Puteh, Mohd Hairul Khamidun, Abdull Rahim Mohd Yusoff, Noorul Hudai Abdullah, Noraziah Ahmad, Zainab Mat Lazim, and Maria Nuid. "Adsorption of phosphate from aqueous solution onto iron-coated waste mussel shell: Physicochemical characteristics, kinetic, and isotherm studies." *Biointerface Research in Applied Chemistry* 11 (2021): 12831-12842. https://doi.org/10.33263/BRIAC115.1283112842

[4] Wang, Huan, Jorge García Molinos, Jani Heino, Huan Zhang, Peiyu Zhang, and Jun Xu. "Eutrophication causes invertebrate biodiversity loss and decreases cross-taxon congruence across anthropogenically-disturbed lakes." *Environment International* 153 (2021): 106494. https://doi.org/10.1016/j.envint.2021.106494

[5] Huang, Xiang Long, Feiyun Zhao, Yu Qi, Yun-Ao Qiu, Jun Song Chen, Hua Kun Liu, Shi Xue Dou, and Zhiming M. Wang. "Red phosphorus: A rising star of anode materials for advanced K-ion batteries." *Energy Storage Materials* 42 (2021): 193-208. https://doi.org/10.1016/j.ensm.2021.07.030

[6] Migliavacca, Daniela Montanari, Elba Calesso Teixeira, Fernanda Gervasoni, Rommulo Vieira Conceição, and Maria Teresa Raya Rodriguez. "Characterization of wet precipitation by X-ray diffraction (XRD) and scanning electron microscopy (SEM) in the metropolitan area of Porto Alegre, Brazil." *Journal of Hazardous Materials* 171, no. 1-3 (2009): 230-240. https://doi.org/10.1016/j.jhazmat.2009.05.135

[7] Nandiyanto, Asep Bayu Dani, Rosi Oktiani, and Risti Ragadhita. "How to read and interpret FTIR spectroscope of organic material." *Indonesian Journal of Science and Technology* 4, no. 1 (2019): 97-118. https://doi.org/10.17509/ijost.v4i1.15806

[8] Pettersson, Pontus, and Andreas Barth. "Correlations between the structure and the vibrational spectrum of the phosphate group. Implications for the analysis of an important functional group in phosphoproteins." *RSC Advances* 10, no. 8 (2020): 4715-4724. https://doi.org/10.1039/C9RA10366J

[9] Zou, Shuai-Wen, Kok Yuen Koh, Zhihao Chen, Yu-Yang Wang, J. Paul Chen, and Yu-Ming Zheng. "Adsorption of organic and inorganic arsenic from aqueous solution: Optimization, characterization and performance of Fe-Mn-Zr ternary magnetic sorbent." *Chemosphere* 288 (2022): 132634. https://doi.org/10.1016/j.chemosphere.2021.132634

[10] Howard, K. T., G. K. Benedix, P. A. Bland, and G. Cressey. "Modal mineralogy of CM chondrites by X-ray diffraction (PSD-XRD): Part 2. Degree, nature and settings of aqueous alteration." *Geochimica et Cosmochimica Acta* 75, no. 10 (2011): 2735-2751. https://doi.org/10.1016/j.gca.2011.02.021

[11] Liu, Tao, Xu Chen, Xin Wang, Shourong Zheng, and Liuyan Yang. "Highly effective wastewater phosphorus removal by phosphorus accumulating organism combined with magnetic sorbent MFC@La(OH)$_3$." *Chemical Engineering Journal* 335 (2018): 443-449. https://doi.org/10.1016/j.cej.2017.10.117

[12] Jeon, Dong Jin, and Sung Ho Yeom. "Recycling wasted biomaterial, crab shells, as an adsorbent for the removal of high concentration of phosphate." *Bioresource Technology* 100, no. 9 (2009): 2646-2649. https://doi.org/10.1016/j.biortech.2008.11.035

[13] Xiong, Jibing, Yong Qin, Ejazul Islam, Min Yue, and Wenfeng Wang. "Phosphate removal from solution using powdered freshwater mussel shells." *Desalination* 276, no. 1-3 (2011): 317-321. https://doi.org/10.1016/j.desal.2011.03.066

[14] Shen, Youhao, Linlan Zhuang, Jian Zhang, Jinlin Fan, Ting Yang, and Shuo Sun. "A study of ferric-carbon micro-electrolysis process to enhance nitrogen and phosphorus removal efficiency in subsurface flow constructed wetlands." *Chemical Engineering Journal* 359 (2019): 706-712. https://doi.org/10.1016/j.cej.2018.11.152

[15] Luo, Pei, Feng Liu, Xinliang Liu, Xiao Wu, Ran Yao, Liang Chen, Xi Li, Runlin Xiao, and Jinshui Wu. "Phosphorus removal from lagoon-pretreated swine wastewater by pilot-scale surface flow constructed wetlands planted with Myriophyllum aquaticum." *Science of the Total Environment* 576 (2017): 490-497. https://doi.org/10.1016/j.scitotenv.2016.10.094

[16] Lee, Jae-In, Jeong-Man Kim, Soo-Cheul Yoo, Eun Hea Jho, Chang-Gu Lee, and Seong-Jik Park. "Restoring phosphorus from water to soil: Using calcined eggshells for P adsorption and subsequent application of the adsorbent as a P fertilizer." *Chemosphere* 287 (2022): 132267. https://doi.org/10.1016/j.chemosphere.2021.132267

[17] Paradelo, R., M. Conde-Cid, L. Cutillas-Barreiro, M. Arias-Estévez, J. C. Nóvoa-Muñoz, E. Álvarez-Rodríguez, M. J. Fernández-Sanjurjo, and A. Núñez-Delgado. "Phosphorus removal from wastewater using mussel shell: Investigation on retention mechanisms." *Ecological Engineering* 97 (2016): 558-566. https://doi.org/10.1016/j.ecoleng.2016.10.066

[18] Nguyen, T. A. H., H. H. Ngo, W. S. Guo, T. H. H. Nguyen, S. Soda, N. D. Vu, T. K. A. Bui et al. "White hard clam (Meretrix lyrata) shells media to improve phosphorus removal in lab-scale horizontal sub-surface flow constructed wetlands: Performance, removal pathways, and lifespan." *Bioresource Technology* 312 (2020): 123602. https://doi.org/10.1016/j.biortech.2020.123602

[19] Nguyen, T. A. H., H. H. Ngo, W. S. Guo, T. T. Nguyen, N. D. Vu, S. Soda, T. H. H. Nguyen et al. "White hard clam (Meretrix lyrata) shells as novel filter media to augment the phosphorus removal from wastewater." *Science of the Total Environment* 741 (2020): 140483. https://doi.org/10.1016/j.scitotenv.2020.140483

[20] Babapour, Mohammad, Mohammad Hadi Dehghani, Mahmood Alimohammadi, Masomeh Moghadam Arjmand, Mehdi Salari, Leila Rasuli, Nabisab Mujawar Mubarak, and Nadeem Ahmad Khan. "Adsorption of Cr (VI) from aqueous solution using mesoporous metal-organic framework-5 functionalized with the amino acids: Characterization, optimization, linear and nonlinear kinetic models." *Journal of Molecular Liquids* 345 (2022): 117835. https://doi.org/10.1016/j.molliq.2021.117835

[21] Yan, Yubo, Xiuyun Sun, Fangbian Ma, Jiansheng Li, Jinyou Shen, Weiqing Han, Xiaodong Liu, and Lianjun Wang. "Removal of phosphate from etching wastewater by calcined alkaline residue: Batch and column studies." *Journal of the Taiwan Institute of Chemical Engineers* 45, no. 4 (2014): 1709-1716. https://doi.org/10.1016/j.jtice.2013.12.023

[22] Wu, Feng-Chin, Ru-Ling Tseng, Shang-Chieh Huang, and Ruey-Shin Juang. "Characteristics of pseudo-second-order kinetic model for liquid-phase adsorption: A mini-review." *Chemical Engineering Journal* 151, no. 1-3 (2009): 1-9. https://doi.org/10.1016/j.cej.2009.02.024

[23] Salim, Nur Atikah Abdul, Mohamad Ali Fulazzaky, Muhammad Abbas Ahmad Zaini, M. H. Puteh, M. H. Khamidun, A. R. M. Yusoff, N. H. Abdullah, N. Ahmad, Z. M. Lazim, and M. Nuid. "Phosphate removal from wastewater in batch system using waste mussel shell." *Biointerface Research in Applied Chemistry* 11, no. 4 (2021): 11473-11486.

[24] Binh, Quach An, and Hong-Hai Nguyen. "Investigation the isotherm and kinetics of adsorption mechanism of herbicide 2, 4-dichlorophenoxyacetic acid (2, 4-D) on corn cob biochar." *Bioresource Technology Reports* 11 (2020): 100520. https://doi.org/10.1016/j.biteb.2020.100520

[25] Simonin, Jean-Pierre. "On the comparison of pseudo-first order and pseudo-second order rate laws in the modeling of adsorption kinetics." *Chemical Engineering Journal* 300 (2016): 254-263. https://doi.org/10.1016/j.cej.2016.04.079

[26] Salim, Nur Atikah Abdul, Mohd Hafiz Puteh, Abdull Rahim Mohd Yusoff, Noorul Hudai Abdullah, Mohamad Ali Fulazzaky, Mohd A'ben Zulkarnain Rudie Arman, Mohd Hairul Khamidun et al. "Adsorption isotherms and kinetics of phosphate on waste mussel shell." *Malaysian Journal of Fundamental and Applied Sciences* 16, no. 3 (2020): 393-399. https://doi.org/10.11113/mjfas.v16n3.1752

[27] You, Kai, Wenke Yang, Ping Song, Liwei Fan, Shuyi Xu, Bingying Li, and Lei Feng. "Lanthanum-modified magnetic oyster shell and its use for enhancing phosphate removal from water." *Colloids and Surfaces A: Physicochemical and Engineering Aspects* 633 (2022): 127897. https://doi.org/10.1016/j.colsurfa.2021.127897

[28] Kabir, Mohammad Mahbub, Mst Mahmoda Akter, Shahjalal Khandaker, Brandon H. Gilroyed, Md Didar-ul-Alam, Mahmuda Hakim, and Md Rabiul Awual. "Highly effective agro-waste based functional green adsorbents for toxic chromium (VI) ion removal from wastewater." *Journal of Molecular Liquids* 347 (2022): 118327. https://doi.org/10.1016/j.molliq.2021.118327

[29] Abdullah, Noorul Hudai, Mohamad Syahrul Syazwan Yaacob, Nur Athirah Iliyani Rani, Tuan Muhammad Fikri Haziq Tuan Azman, Muhammad Nur Iqbal Sumawan, Nor Baizura Hamid, Nur Atikah Abdul Salim, Masiri Kaamin, Muhammad Azraie Abdul Kadir, Noraziah Ahmad, Zainab Mat Lazim, Maria Nuid, and Amirreza Talaiekhoza. "Phosphate Adsorption from Synthetic Aqueous Solutions by Waste Mussel Shell: Kinetics and Isotherms Studies." *International Journal of Nanoelectronics and Materials* 14 (2021): 9.

[30] Mohan, Dinesh, and Charles U. Pittman Jr. "Arsenic removal from water/wastewater using adsorbents-a critical review." *Journal of Hazardous Materials* 142, no. 1-2 (2007): 1-53. https://doi.org/10.1016/j.jhazmat.2007.01.006

[31] Khayyun, Thair Sharif, and Ayad Hameed Mseer. "Comparison of the experimental results with the Langmuir and Freundlich models for copper removal on limestone adsorbent." *Applied Water Science* 9, no. 8 (2019): 170. https://doi.org/10.1007/s13201-019-1061-2

[32] Zhu, Mengyuan, Jingqi Dai, Rui Liu, Jiuping Xu, and Aladdin Alwisy. "Two-period based carbon-economy equilibrium strategy for modular construction supply planning." *Journal of Cleaner Production* 290 (2021): 125674. https://doi.org/10.1016/j.jclepro.2020.125674

[33] Firdous, Rafia, Tamino Hirsch, Detlef Klimm, Barbara Lothenbach, and Dietmar Stephan. "Reaction of calcium carbonate minerals in sodium silicate solution and its role in alkali-activated systems." *Minerals Engineering* 165 (2021): 106849. https://doi.org/10.1016/j.mineng.2021.106849

[34] Low, Wei Chian, Khai Ching Ng, and Hoon Kiat Ng. "Verification of Lattice Spring Model for Modelling Composite Material." *Journal of Advanced Research in Applied Mechanics* 97, no. 1 (2022): 1-6. https://doi.org/10.37934/aram.97.1.16